Structural analysis of the adenovirus type 2 E3/19K protein using mutagenesis and a panel of conformation-sensitive monoclonal antibodies

Beatrice Menz[a+], Martina Sester[b], Katja Koebernick[a+], Ralf Schmid[c] and Hans-Gerhard Burgert[a*]

[a]Department of Biological Sciences, University of Warwick, Coventry CV4 7AL, UK

[b]Department of Internal Medicine IV, University of the Saarland, 66421 Homburg, Germany

[c]Department of Biochemistry, University of Leicester, Leicester LE1 9HN, UK

[+]Current addresses: BM, Birkhäuser Verlag AG, Viaduktstraße 42, 4051 Basel**,** Switzerland

KK, Institute for Biochemistry, Department of Developmental Biochemistry, University of Göttingen, 37077 Göttingen, Germany

[*] Corresponding author. Tel.: +44 2476524744.
E-mail address: H-G.Burgert@warwick.ac.uk (H.-G. Burgert)

Total number of words in the main text: 5955, excl. references and Fig. legends

Total number of words in the Summary: 279

Total number of figures and tables: 8 figures, 1 table

Abstract

The E3/19K protein of human adenovirus type 2 (Ad2) was the first viral protein shown to interfere with antigen presentation. This 25 kDa transmembrane glycoprotein binds to MHC class I molecules in the endoplasmic reticulum (ER), thereby preventing transport of newly synthesized peptide-MHC complexes to the cell surface and consequently T cell recognition. Recent data suggest that E3/19K also sequesters MHC class I like ligands intracellularly to suppress NK cell recognition. While the mechanism of ER retention is well understood, the structure of E3/19K remains elusive. To further dissect the structural and antigenic topography of E3/19K we carried out site-directed mutagenesis and raised monoclonal antibodies (mAbs) against a recombinant version of Ad2 E3/19K comprising the lumenal domain followed by a C-terminal histidine-tag. Using peptide scanning, the epitopes of three mAbs were mapped to different regions of the lumenal domain, comprising amino acids 3-13, 15-21 and 41-45, respectively. Interestingly, mAb 3F4 reacted only weakly with wild-type E3/19K, but showed drastically increased binding to mutant E3/19K molecules, e.g. those with disrupted disulfide bonds, suggesting that 3F4 can sense unfolding of the protein. MAb 10A2 binds to an epitope apparently buried within E3/19K while that of 3A9 is exposed. Secondary structure prediction suggests that the lumenal domain contains six β-strands and an α-helix adjacent to the transmembrane domain. Interestingly, all mAbs bind to non-structured loops. Using a large panel of E3/19K mutants the structural alterations of the mutations were determined. With this knowledge the panel of mAbs will be valuable tools to further dissect structure/function relationships of E3/19K regarding down regulation of MHC class I and MHC class I like molecules and its effect on both T cell and NK cell recognition.

Keywords: Adenovirus E3/19K; immune evasion; monoclonal antibody epitope mapping; antigen presentation.

1. Introduction

Human adenoviruses (Ads) typically cause acute disease of the eyes, the respiratory tract, and the gastrointestinal tract (Wold and Horwitz, 2007). It is well known that Ads, in particular members of species C including Ad2 and Ad5, can also establish persistent infections (Fox et al., 1977). Infections are facilitated by immunomodulatory proteins that counteract or evade the host immune response (Burgert et al., 2002). Many of these immune evasion proteins are encoded in the early transcription unit 3 (E3) which is dispensable for virus replication in tissue culture cells but is preserved in all human Ads (Burgert et al., 2002; Windheim et al., 2004). E3 proteins have been shown to modulate a variety of immune response mechanisms (Burgert and Blusch, 2000; Burgert et al., 2002; Elsing and Burgert, 1998; Lichtenstein et al., 2004; McNees and Gooding, 2002; McSharry et al., 2008). The most abundant E3 protein of species C Ads, E3/19K, interferes with transport of major histocompatibility (MHC) class I molecules (in human called HLA) and the MHC class I related molecules MICA/B to the cell surface (Burgert and Kvist, 1985; Cox et al., 1991; McSharry et al., 2008). The latter serve as ligands for the activating receptor NKG2D (Lodoen and Lanier, 2005). Consequently E3/19K inhibits recognition by both cytotoxic T lymphocytes and natural killer (NK) cells (Andersson et al., 1987; Burgert and Kvist, 1985; Burgert et al., 1987; Cox et al., 1991; McSharry et al., 2008; Rawle et al., 1989; Tanaka and Tevethia, 1988). In line with in vitro data, results generated in animal models strongly support an immunomodulatory function of E3 proteins *in vivo* (Bruder et al., 1997; Ginsberg et al., 1989; von Herrath et al., 1997).

E3/19K is an intracellular transmembrane glycoprotein (Ahmed et al., 1982; Persson et al., 1980; Wold et al., 1985). The mature form of Ad2 E3/19K is derived from a precursor of 159 amino acids by cleaving off a 17 amino acid signal sequence. Down-regulation of MHC class I molecules from the cell surface is accomplished by the combined activity of two functional modules in E3/19K, one for recruiting newly synthesized HLA molecules and a second one

for localization in the endoplasmic reticulum (ER) (Burgert and Kvist, 1985; Cox et al., 1991; Nilsson et al., 1989). The ability to localize to the ER has been linked to an ER retrieval signal in the cytoplasmic tail of E3/19K (Jackson et al., 1990; Jackson et al., 1993).

The association between E3/19K and MHC class I molecules is non-covalent and does neither require N-linked carbohydrates, present at amino acid positions 12 and 61 in Ad2 E3/19K (Burgert and Kvist, 1987; Kornfeld and Wold, 1981) nor its cytoplasmic tail (Cox et al., 1991; Pääbo et al., 1987; Pääbo et al., 1986b). The transmembrane segment might be necessary for HLA interaction within the cell but is not required *in vitro* (Gabathuler et al., 1990; Liu et al., 2005; Pääbo et al., 1986b). Hence, the interaction is primarily mediated by the lumenal portion of E3/19K (Hermiston et al., 1993; Liu et al., 2005; Pääbo et al., 1986b; Sester and Burgert, 1994) which contains two intramolecular disulfide bonds that are absolutely critical for HLA binding (Sester and Burgert 1994). Using hybrid MHC molecules containing domains from E3/19K-binding and non-binding MHC alleles, the polymorphic peptide binding domains α1 and α2 of MHC molecules have been shown to be critical for complex formation with E3/19K (Beier et al., 1994; Burgert and Kvist, 1987; Feuerbach et al., 1994; Jefferies and Burgert, 1990). Site-directed mutagenesis of MHC class I molecules and antibody binding studies suggest that the contact site is formed or influenced by amino acids within the amino-terminal part of the α1-helix and the carboxy-terminal part of the α2-helix at the junction to α3 (Feuerbach et al., 1994; Flomenberg et al., 1994; Liu et al., 2007). The latter putative attachment site is reminiscent of that defined in HLA-A2 for the CMV protein US2 which also interferes with antigen presentation (Gewurz et al., 2001). Binding of E3/19K seems to occur early in the MHC class I assembly pathway even before the α1 and α2 domain are properly folded, possibly during interaction of MHC molecules with calnexin (Sester et al., 2000). However, E3/19K may also retain certain MHC alleles by interfering with TAP-mediated peptide loading (Bennett et al., 1999).

While the sequences of the E3/19K homologous proteins of Ad species B, C, D and E (Burgert et al., 2002; Deryckere and Burgert, 1996) are remarkably diverse, the ability to bind to and to inhibit HLA transport is preserved (Burgert and Blusch, 2000; Burgert et al., 2002; Deryckere and Burgert, 1996; Flomenberg et al., 1992; Pääbo et al., 1986a). Only 20 of the 139-151 amino acids present in E3/19K homologues of different serotypes are strictly conserved, including four cysteines. We previously showed that these conserved cysteines form two intramolecular disulfide bonds between positions 11/28 and 22/83, respectively, which are absolutely required for functional activity (McSharry et al., 2008; Sester and Burgert, 1994). In addition, a relatively conserved stretch of amino acids adjacent to the transmembrane segment has been proposed to be important for HLA association, possibly by influencing correct folding of more distal portions of the molecule (Flomenberg et al., 1992). Loss of HLA binding in mutant E3/19K molecules with in-frame deletions covering the lumenal domain confirmed its crucial role for HLA binding (Hermiston et al., 1993), although gross structural changes, e.g. due to lack of disulfide bond formation (Sester and Burgert, 1994), could not be excluded. Indeed, most of these mutants had lost binding of the conformation-dependent monoclonal antibody (mAb) Tw1.3, indicating extensive structural changes. Thus, more reagents to assess the structural consequences of mutations would be very useful for further functional analysis.

To gain further insight into the structure of E3/19K and to enable controlled mutagenesis studies, we have raised new mAbs directed to its lumenal domain. Their epitopes were identified and found to represent loop regions mostly connecting beta-strands as determined by secondary structure prediction. Differential binding of these mAbs to E3/19K mutants in which conserved amino acids were replaced by serine or alanine revealed the influence of these mutations on structure and folding of the protein.

2. Material and methods

2.1. Construction, expression and purification of His-tagged E3/19K

A truncated form of the Ad2 E3/19K protein containing amino acids 1-108 and a C-terminal histidine tag was produced by PCR-mediated oligonucleotide-directed mutagenesis. The histidine tag was positioned at the C-terminus of the E3/19K construct as this part is normally inserted in the lipid bilayer and does not appear to be directly involved in complex formation with HLA (Cox et al., 1991; Flomenberg et al., 1992; Gabathuler et al., 1990; Pääbo et al., 1986b). As template for *in vitro* mutagenesis and for generation of the expression construct, the *Eco*RI D fragment of the Ad2 genome (2674bp, comprising nucleotides 27372-30046) was used which had been inserted into the *Eco*RI site of Bluescript II KS- (Sester and Burgert, 1994). The 5´ oligonucleotide contained an *Nco*I restriction site followed by an ATG start codon and a codon for alanine, the first amino acid of the mature protein omitting the signal sequence (*Nco*I primer: 5´-GGCGCCATGGCCAAAAAGGTTGAGTT-TAAG-3´). The 3´ oligonucleotide contained the codons for amino acids 104-108, followed by a *Bgl*II restriction site which at the same time changed the codon TGT of Cys-109 to AGA for arginine (*Bgl*II oligonucleotide: 5´-AGGGAGATCTAAAGGTGCCAG-TGTTCTC-3´). The purified PCR product was digested with *Nco*I and *Bgl*II, and ligated into *Nco*I/*Bgl*II cleaved pQE60 (Qiagen). The pQE expression construct was transfected into *E. coli* M15 (pREP4). Transformants were selected with ampicillin and kanamycin and were screened by preparing small-scale expression cultures upon induction with 2 mM IPTG. Bacteria were solubilized in 8M urea, 0.1 M sodium phosphate, 0.01 M Tris/HCl pH8.0, the lysate was cleared by centrifugation and applied on a nickel chelate column, which was washed sequentially with 8 M urea, 0.1 M sodium phosphate, 0.01 M Tris/HCl pH 6.3, and 0.1 M Tris/HCl pH8.0. Finally, the histidine-tagged protein was eluted with 0.1 M Tris/0.1 M EDTA pH8.0.

2.2. Cell lines, culture conditions and virus infection

293 cells stably expressing wild-type E3/19K of Ad2 (293E3-45), cysteine to serine replacement mutants and Ala-22 with an alanine substitution of C22 have been described (Körner et al., 1992; Sester and Burgert, 1994). Cell lines transfected with mutants E5, P9, T14, K27, I37, K42, W52, G55, Y60, V62, V64, M87, and W96 were constructed by replacing the codon for the respective amino acid by an alanine codon (to be published elsewhere). Culture of A549 (human lung carcinoma, ATCC CCL 185) and 293 cells, transfection and subsequent selection was performed as described (Hilgendorf et al., 2003; Sester and Burgert, 1994). Infection with Ad2 and Ad5 was carried out as described using an MOI of ~50 (Hilgendorf et al., 2003). Sp2/0-Ag14 myeloma cells (ATCC CRL 1581) and antibody-producing hybridoma cells were cultured in RPMI 1640 containing 10% fetal calf serum, glutamine and antibiotics.

2.3. Immunization of mice and production of mAbs

Three C3H and three BALB/c mice were immunized subcutaneously with 25 µg of purified His-E3/19K in complete Freund´s adjuvant and subsequently boosted twice with the same amount of protein in incomplete Freund´s adjuvant. Sera were tested for E3/19K-specific reactivity using an ELISA employing recombinant His-tagged E3/19K as test antigen, and immunoprecipitations of 293E3-45 cell lysates. Only C3H mice were used for further studies. The last immunization was done three days before fusion of spleen cells with SP2 cells, essentially as described (Köhler and Milstein, 1975). The supernatants of the resulting hybridomas were initially screened by ELISA. Subclass determination was done using a mouse mAb isotyping kit (Sigma Immuno Type^{TM}, Sigma). All antibodies newly described here are of IgG1 type and bind to protein A.

2.4. ELISA

Purified His-E3/19K (1 µg/well) was adsorbed overnight to Maxisorp plates (Nunc, Denmark) in 100 mM carbonate/bicarbonate buffer pH9.6 at 4°C. Thereafter, plates were blocked for 1h at room temperature with blocking solution (PBS/5% nonfat milk powder). 100 µl of culture supernatants or diluted sera were added per well and left for 2 h at room temperature. Plates were washed three times with blocking solution before 50 µl horseradish peroxidase (HRP)-conjugated rabbit anti-mouse (DAKO, Germany) was added (1:2500 in blocking solution). After 2 h, the plates were washed three times with blocking solution and once with PBS. As substrate, 0.03% o-phenylenediamine in 25 mM citric acid/25 mM K_2HPO_4/0.01% H_2O_2 was added. Colour development was stopped with 3 M HCl, and the optical density was measured at 490 nm. MAb Tw1.3, kindly provided by Dr. J. Yewdell (NIH), was used as positive control for the assays (Cox et al., 1991).

2.5. Antibody inhibition assay

Maxisorp plates (Nunc) adsorbed overnight with purified His-E3/19K as above were incubated with increasing amounts of E3/19K-specific mAbs per well. After washing twice with blocking solution, radiolabelled mAbs were added and incubated for 2 h, followed by another three washes. The amount of bound radioactive mAb was determined by solubilizing the proteins with 10% SDS and counting in a β-counter. For labelling of mAbs with ^{35}S-methionine, $5x10^6$ antibody-producing cells were starved for 30 min in methionine-free medium and then incubated with 500 µCi ^{35}S-methionine (Redivue, GE Healthcare) for 4h. Cells were pelleted and the labelled antibodies separated from free ^{35}S-methionine by gel filtration.

2.6. Epitope mapping

Epitope mapping using overlapping 13mer peptides encompassing the E3/19K sequence from amino acid 1 to 108 was carried out by Jerini AG, Germany. Briefly, a total of 49 13mer peptides with an overlap of 11 amino acids were synthesized directly on a cellulose membrane by SPOT synthesis. After blocking, the cellulose-bound peptide library was incubated sequentially with 1 μg/ml of mAbs (2, 4 and 12μg/ml were used for Tw1.3) and was then washed with T-TBS (31 mM Tris pH8, 170 mM NaCl, 6.4 mM KCL, 0.05% Tween 20). Bound antibodies were electrotransferred onto PVDF membranes (Millipore) by fractionated blotting using a semi-dry blotter. Membranes were probed with the mAbs and bound mAbs were visualized by HRP-conjugated anti-mouse IgG/ECL.

2.7. Radioactive labelling of cells, immunoprecipitation and SDS-PAGE

Labelling with ^{35}S-methionine (Redivue, GE Healthcare), immunoprecipitation, tunicamycin treatment and SDS-PAGE were carried out essentially as described previously (Burgert and Kvist, 1985; Burgert et al., 1987). The rabbit anti-E3/19K serum Ctail was raised against the cytoplasmic tail of Ad2 E3/19K (Sester and Burgert, 1994). For comparison, the mAb Tw1.3 (Cox et al., 1991) which recognizes E3/19K from Ad2 and Ad5 was included. Radioactive proteins were quantified by PhosphorImager (BAS 1000, Fujix) analysis.

2.8. Western blot analysis

Immunoprecipitated material was run on 12% SDS-PAGE minigels and blotted on to Hybond ECL nitrocellulose membranes for 1 h at 100V in 25 mM Tris, 192 mM glycine buffer pH8.3 containing 20% (v/v) methanol using the protean system (Bio-Rad). Non-specific binding sites on the membrane were blocked for one hour in ELISA blocking solution. The membrane was then incubated for 2 h with culture supernatants of the respective antibodies diluted in blocking solution. After several washes, the membrane was incubated for another 2 h with

peroxidase-conjugated Affipure Fab-fragment (goat anti-mouse IgG H+L chain, Dianova, Germany) diluted 1:4000 in blocking solution. After washing with several changes of blocking solution and one wash in TBS/0.1% Tween, the blot was developed using ECL substrate (GE Healthcare) and subsequently exposed on Hyperfilm ECL autoradiography film.

2.9. Bioinformatics

Homologous sequences to Ad2 were retrieved from the results of a BLAST (Altschul et al., 1990) similarity search against the UniProt (The_UniProt_Consortium, 2007) database at the EBI BLAST-server and aligned using MUSCLE (Edgar, 2004). Jpred (Cole et al., 2008), PSIPRED (Bryson et al., 2005) and the PredictProtein server (Rost et al., 2004) were used to predict the secondary structure of Ad2. For the prediction of transmembrane helices PHDhtm (Rost et al., 1996) and TMHMM (Krogh et al., 2001) were employed. For further structure prediction the full Ad2 sequence and truncated versions lacking the predicted transmembrane helix and/or signal peptide were submitted to the Genesilico fold recognition meta-server (Kurowski and Bujnicki, 2003).

3. Results

3.1. Monoclonal antibodies raised against recombinant E3/19K specifically recognize E3/19K of Ad2

Spleens of mice immunized with recombinant His-tagged E3/19K were used to produce hybridomas. Hybridoma supernatants were screened by ELISA for reactivity with E3/19K-His (data not shown). Hybridomas testing positive were re-tested after subcloning and three clones (3A9, 3F4, and 10A2) were used for further analysis. The conformation-sensitive mAb Tw1.3 was used as a control (Cox et al., 1991). Supernatants of clones 3A9 and 3F4 proved positive in immunoprecipitation using lysates of 293E3-45 cells constitutively expressing E3/19K (data not shown). Antibodies secreted by these clones also precipitated E3/19K from A549 cells that had been infected with Ad2 prior to metabolic labelling with ^{35}S-methionine (Fig. 1A). Unlike mAb Tw1.3, which recognizes the highly homologous E3/19K proteins of Ad2 and Ad5, 3A9 and 3F4 were specific for Ad2 E3/19K (Fig. 1A). MAb 10A2 did not precipitate the protein, however, western blotting of E3/19K from infected A549 cells revealed its reactivity with denatured Ad2 E3/19K but not Ad5 E3/19K (Fig. 1B). Since none of the three mAbs reacted with the corresponding protein of Ad5, the epitopes recognized by these antibodies must comprise sequences that are unique to Ad2 E3/19K. The reactivity of mAb 3A9 seemed to be similar to that of mAb Tw1.3 while the amount of E3/19K precipitated by mAb 3F4 was only about 10% of that of mAb Tw1.3. Thus, 3F4 either binds the native molecule only with low affinity, or alternatively, may bind to a proportion of E3/19K molecules that are partially unfolded and hence accessible for binding.

3.2. Peptide-mapping identifies the minimal epitopes of the mAbs

All three monoclonal antibodies were able to detect E3/19K on western blots. In contrast to the epitope recognized by mAb Tw1.3, reducing conditions (for mAb 10A2, see Fig. 1B, lane

3; and data not shown) did not abolish detection. This suggested that the epitopes of these new mAbs are continuous rather than conformational. This prompted us to identify the epitopes using a peptide-based epitope mapping strategy. A set of 49 overlapping 13mer-peptides representing the entire lumenal domain of E3/19K, plus a few amino acids of the transmembrane region (amino acids 1-108) were synthesized by SPOT synthesis on a cellulose membrane. The peptide scan showed that mAb 10A2 reacted with peptides 1 and 2, mAb 3A9 with peptides 5-8, and mAb 3F4 with peptides 17-21. The respective consensus sequences comprise amino acids 3-13 for mAb 10A2, 15-21 for mAb 3A9, and 41-45 for mAb 3F4 (Fig. 2). For mAb Tw1.3 no significant reactivity was detected in this screen (data not shown), consistent with the notion that this antibody recognizes a discontinuous epitope. Together with the fact that the mAbs were specific for Ad2 E3/19K, these results allowed us to identify the crucial amino acids within each epitope. The 3A9 epitope comprises the sequence F<u>KS</u>EANE in Ad2. As the Ad5 protein with the corresponding sequence FAAEANE is not recognized, amino acids K and S are critical for reactivity. In an analogous manner, the crucial residue of the 3F4 epitope was identified as D in position 41 since the single amino acid difference in position 41 abrogated reactivity to the Ad5 protein (<u>D</u>KIGKY in Ad2 versus NKIGKY in Ad5). The 10A2 epitope encompasses the sequence KV<u>E</u>FKEPACN in Ad2 while the corresponding sequence in Ad5 is KVDFKEPACN. Therefore, E in position 5 seems critical for 10A2 reactivity. As 10A2 did not bind to Ad2 E3/19K in immunoprecipitation experiments, but recognized the protein on western blots and with higher reactivity after reduction (Fig. 1B), the epitope appears to be inaccessible unless the molecule is at least partially unfolded. In line with this view, 10A2 can recognize E3/19K mutants with disrupted C11/C28 bridge using flow cytometry in the presence of 0.075% saponin (data not shown).

3.3. Monoclonal antibodies differentially recognize cysteine replacement mutants

Ad2 E3/19K contains a total of seven cysteines. Four of these are conserved among Ads and form two disulfide bridges between C11/C28 and C22/C83, respectively. Serine substitution of these cysteines reduced (C22 and C83) or abolished (C11 and C28) Tw1.3 binding. Binding studies using the additional mAbs with known epitopes and wild-type and mutant forms of E3/19K should yield important information as to the structure of the wild-type molecule and the structural changes induced by the mutations. Therefore, quantitative immunoprecipitation experiments with mAbs Tw1.3, 3F4 and 3A9 were carried out using cell lines stably expressing wild-type E3/19K (293E3) and E3/19K with individual cysteines mutated to serine or alanine (Ala-22; Fig. 3A-C). Ala-22 was included, because replacement of this amino acid by serine creates an additional site for N-glycosylation (Sester and Burgert, 1994), as demonstrated by the slower migration of the C22S mutant 22 (Fig. 3B, lanes 5-8). The amounts of wild-type and mutant E3/19K precipitated were determined and related to that precipitated with Ctail serum, as previously described (Sester and Burgert, 1994), the binding of which was unaffected by the mutations. MAb 10A2 proved negative with wild-type E3/19K and all mutants under immunoprecipitation conditions (data not shown). The relative binding of mAbs to the different mutants is expressed as the ratio of radioactivity detected by mAbs versus that by Ctail, with the ratio obtained for wild-type E3/19K set to 1 (Fig. 4).

As for Tw1.3 (Fig. 4, top), binding of 3A9 was abrogated in mutants C11 and C28, whereas its binding of C22 and C83 was essentially unaffected. Reactivity of 3A9 to Ala-22, C101, C109 and C122 was slightly reduced (Fig. 4). Since binding of 3A9 depends on an intact disulfide bond between C11 and C28, this antibody may serve as indicator for the presence of this structural entity in E3/19K mutants with amino acid changes in positions other than these cysteines.

Interestingly, 3F4 exhibited a binding pattern reciprocal to that of Tw1.3. Binding of the C11 and C28 mutants by this antibody increased 10 and 15 fold, respectively, as compared to wild-type E3/19K, while binding of mutants C22, Ala-22 and C83 was increased to 5.4, 3.6 and 4 fold, respectively (Fig. 4). Although the absolute amount of the C11, C28 and C22 mutants precipitated in this experiment was small (Fig. 3), the profound relative increase to Ctail suggests that the 3F4 epitope becomes exposed upon unfolding. Precipitation of mutants C101, C109 and C122 by 3F4 was within the same range as binding to wild-type E3/19K (Fig. 4). The concordant changes in mAb binding for mutant pairs C11 and C28 as well as C22/Ala-22 and C83 corroborate our previous findings that these cysteine pairs form intramolecular disulfide bonds in the native molecule.

3.4. Competitive binding of monoclonal antibodies Tw1.3 and 3A9

Due to the similar binding properties of 3A9 and Tw1.3, we tested whether these mAbs compete for binding to E3/19K using a radioactive competition assay (Fig. 5). Unlabelled mAb 3F4 was included as negative control. Fig. 5A shows the binding of radioactively labelled mAb Tw1.3 to E3/19K after preincubation with increasing amounts of unlabelled mAbs. As expected, preincubation with unlabelled Tw1.3 led to a drastic reduction of binding by labelled Tw1.3, whereas preincubation with 3F4 did not. Binding of Tw1.3 was also significantly reduced by preincubation with 3A9 (by ~30% at the highest 3A9 concentration). By contrast, binding of radiolabelled 3A9 could only be inhibited by 3A9 itself but neither by 3F4 nor by Tw1.3 (Fig. 5B). Thus, Tw1.3 binding to a conformational epitope is affected by prior binding of 3A9 to amino acids 15-21 whereas prior Tw1.3 attachment still allows access of 3A9 to its confined epitope.

3.5. Antibody binding is not affected by carbohydrates

As the 10A2 epitope includes the N-linked glycan at position 12 and the 3F4 epitope may be spacially relatively close to the carbohydrate attached at position 61, these glycans may shield the epitope and hence may prevent binding of mAbs to their respective epitopes in the native protein. To address this question, E3/19K positive 293E3-45 cells were labelled with ^{35}S-methionine and treated with tunicamycin, resulting in synthesis of unglycosylated E3/19K. As expected, immunoprecipitation of such molecules (Fig. 6) revealed the unglycosylated form of E3/19K with a M_r of 17 kDa. The relative amount precipitated by Tw1.3 and 3A9 upon tunicamycin treatment was decreased by 40% and 56%, respectively, as compared to that precipitated by Ctail serum (mean of two independent experiments). However, elimination of carbohydrates upon tunicamycin treatment did not rescue binding of 10A2. In agreement, we find that mutant T14, which is not glycosylated at position 12, is also not better recognized by 10A2 (data not shown). Thus, the lack of 10A2 reactivity cannot be explained by masking carbohydrates. By contrast, 3F4 precipitated 1.7 fold more E3/19K upon deglycosylation (data not shown). Although this increase is relatively small compared to the 5-15 fold increase of 3F4 binding seen in E3/19K cysteine replacement mutants, it suggests that access to the 3F4 epitope may be impeded to some extent by carbohydrates.

3.6. Differential binding of mAbs to E3/19K mutants with alanine substitutions of conserved amino acids

Only 20 of the 104 amino acids representing the lumenal domain of Ad2 E3/19K (including C11, C22, C28 and C83) are strictly conserved in E3/19K homologues of species B, C, D and E (Burgert et al., 2002). These conserved residues are predicted to be important for structure and function of the molecule. To examine their role, we have used alanine-scanning mutagenesis to alter these residues. A selected set of mutant E3/19K molecules was stably expressed in 293 cells to assess the effect of these mutations on E3/19K structure by

monitoring binding of mAbs Tw1.3, 3A9 and 3F4 (Fig. 7). Cell lines expressing wild-type and mutant E3/19K were lysed and E3/19K was immunoprecipitated with the different antibodies and the relative amount of E3/19K was quantified as described before (Fig. 3 and 4). Binding of the conformation-dependent mAb Tw1.3 was severely compromised in mutants P9, I37, K42, Y60, V62 and V64. This is likely caused by global structural changes, since we observed a concomitant increase in 3F4 binding in all but the K42 mutant in which the mutated amino acid lies within the 3F4 epitope (Fig. 2). Mutations of W52 and G55, presumably located in the vicinity of the 3F4 binding site, also triggered a strong increase in 3F4 binding, yet did not significantly alter binding to Tw1.3. In mutant K27, Tw1.3 binding remained unaffected, 3F4 binding was lost and that of 3A9 was markedly decreased (~70%). Binding of 3A9 to the other mutants was only marginally affected as compared to that of 3F4 and Tw1.3. Therefore, the epitope recognized by 3A9 seems to be similarly exposed in essentially all of these point mutants. Thus, as the Ctail serum, 3A9 may be very useful to control the expression level of these mutants. The complete set of mAbs with their differential binding properties represents a valuable tool to standardize the expression levels of these mutants when examining the functional alterations induced by the individual mutation.

4. Discussion

Structure-function studies of E3/19K have been hampered by the availability of one single conformation-sensitive mAb, Tw1.3 (Cox et al., 1991). For example, deletion of 4-12 amino acids within the lumenal domain, which abrogated HLA binding was generally accompanied by a loss of Tw1.3 binding (Hermiston et al., 1993). To gain further insight into the structure of E3/19K and to allow further functional studies using E3/19K mutants, a panel of Ad2 E3/19K mutants with mutations in conserved amino acids and a set of new mAbs to Ad2 E3/19K were generated. The minimal epitopes of the new mAbs were identified using peptide scanning and their differential binding to the mutant E3/19K molecules was used to characterize conformational changes associated with single amino acid substitutions of conserved residues. Secondary structure predictions revealed that the mAbs bind to loop regions and overall gave further insight into the potential structure of this paradigmatic viral protein (Fig. 8).

The reactivity of mAb 3A9 is similar to that of mAb Tw1.3 in its efficient recognition of native E3/19K and its dependence on the formation of the disulfide bond between C11 and C28. However, in contrast to Tw1.3 with its conformational epitope, 3A9 is able to bind to a linear sequence and replacement of cysteines at position 22 or 83 did not have any negative effect on recognition (Fig. 3 and 4). The peptide scan identified amino acids 15-21 as minimal epitope of 3A9 (Fig. 2). The ~50% reduced binding of 3A9 to mutant T14 might be expected, as this amino acid lies directly adjacent to the minimal 3A9 epitope and alanine substitution leads to elimination of a carbohydrate. Interestingly, reactivity to K27 was also decreased (by ~75%). Both mutants retain the ability to bind to Tw1.3 and are functionally active (data not shown), indicating that the disulfide bonds are correctly formed and only local structural changes occur. Thus, amino acid K27 either appears to constitute part of the 3A9 epitope or may be required for its accessibility. One likely explanation is that K27 is brought in close

vicinity to the epitope in three dimensional space by formation of the disulfide bridge between C11 and C28 (Fig. 8) as its disruption is associated with the loss of 3A9 reactivity. Consistent with this view, 3A9 can also detect the wild-type protein after denaturation (in Western blots), but reducing conditions drastically diminish its reactivity (data not shown). Alternatively, K27 may influence accessibility of the 3A9 epitope by forming a salt bridge with one of the glutamic acid residues in the epitope. In this case, the lack of recognition of mutants C11 and C28, and reduced binding of T14 and K27 may result from local conformational changes that may mask the epitope. In summary, 3A9 binds to amino acids 15-21, but full reactivity requires a T in position 14 (or a carbohydrate at position 12) and a K in position 27. Thus, although not completely conformation-independent, this antibody is significantly less sensitive to structural changes than Tw1.3 (Fig. 7). Therefore, 3A9 may be used to detect most E3/19K mutants not recognized by Tw1.3.

The minimal 3F4 epitope was mapped to amino acids 41-45. Corroborating the epitope assignment, the K42 mutant completely lost reactivity with 3F4, as did Ad5 E3/19K with N instead of D at position 41. Interestingly, when analysing the cysteine mutants, mAb 3F4 exhibited a reactivity pattern to the cysteine mutants inverse to Tw1.3 (Fig. 4). 3F4 showed only very weak recognition of wild-type E3/19K but disruption of the two conserved disulfide bonds by replacing any of the cysteines at positions 11, 22, 28 or 83 led to a dramatic relative increase in recognition by this antibody. Replacement of the other cysteines did not have any effect. Likewise, mutants P9, I37, Y60, V62 and V64 also showed a drastic increase (~10-20 fold) in 3F4 binding accompanied by a corresponding decrease or loss in binding of Tw1.3. Thus, the 3F4 epitope seems to be largely inaccessible in the wild-type molecule, yet becomes more exposed in these mutants presumably undergoing at least partial unfolding. Intriguingly, secondary structure prediction (Fig. 8) suggests that the conserved amino acids Y60, V62 and V64 face the interior side of a β-strand which supports the notion that mutation of these

residues may cause unfolding thereby affect Tw1.3 binding. Mutants W52 and G55 also showed a profound increase in 3F4 binding but were still bound by Tw1.3, arguing for local structural changes and possibly a close contact of the fourth (the 3F4 epitope) and fifth loop (Fig. 8).

MAb 10A2 recognized peptides containing amino acids 3 to 13 which are predicted to form a non-structured loop. 10A2 neither precipitated wild-type E3/19K nor any of the alanine mutants under immunoprecipitation conditions. We can not exclude the possibility that this is due to a lower binding of 10A2 to protein A. However, 10A2 recognized Ad2 E3/19K in Western blots, with significantly higher efficiency under reducing than non-reducing conditions. Consistent with these data, unfolding of E3/19K by disruption of disulfide bond C11/C28 and to a lesser degree C22/C83 induced reactivity of 10A2 in saponin-treated cells (data not shown). Thus, the epitope appears to be buried inside the native wild-type molecule and may become exposed upon unfolding, particularly upon disruption of the disulfide bonds.

Our data also shed more light on the conformational epitope of mAb Tw1.3. Previous data suggested that amino acids 3-15 and 23-67 in the core flanked by disulfide bond C22/C83 are important for the Tw1.3 epitope (Sester and Burgert, 1994). Since amino acids 3-13 may not be exposed in the native protein as shown by the lack of 10A2 binding in immunoprecipitation, direct contacts of Tw1.3 with this part of the molecule appear to be restricted to amino acids 14-16. In support of the latter, prior binding of 3A9 to amino acids 15-21 reduced that of Tw1.3 by about 30% (Fig. 5). If the 3A9 epitope is adjacent to the N-terminal binding site of Tw1.3, steric hindrance by 3A9 could explain this finding. However, alanine substitution of T14 did not affect the efficiency of immunoprecipitation by Tw1.3 (Fig. 7). Mutations at positions I37 and V64 led to a complete loss of Tw1.3 binding, and mutations at positions P9, I26 (data not shown), K42, Y60, and V62 reduced binding by 45-85%. In these mutants, the disulfide bond between C11 and C28 is preserved as shown by

efficient binding of 3A9 (Fig. 7). We are unable to distinguish whether these amino acids are actual constituents of the Tw1.3 epitope or merely influence the three-dimensional structure to which this antibody binds. The properties of these mAbs are summarised in table 1.

These mAb mapping data were combined with secondary structure predictions and fold recognition (Kurowski and Bujnicki, 2003; Rost and Sander, 1993) (Fig. 8). All secondary structure prediction programmes used consistently suggested six β-strands in the lumenal domain of E3/19K followed by an α-helix in close vicinity to the transmembrane segment that as expected is also predicted to fold as an α-helix. The β-strands in the core domain of E3/19K are connected by short loops (5-9 amino acids). Interestingly, the epitopes of all three mAbs lie within regions that have a high probability of forming loop structures. The N-terminal part (amino acids 3-13) consists of a loop apparently largely buried inside the molecule, which is followed by the first N-linked glycan at N12 and the surface-exposed loop constituting the 3A9 epitope (amino acids 15-21). A less accessible loop between β-strands three and four harbours the 3F4 epitope DKIGK. As the 3F4 signal to peptides 17 and 21 is profoundly reduced compared to peptides 18, 19 and 20 (data not shown) the two amino acids (K and Y) flanking the minimal epitope may also contribute to recognition by 3F4. Thus, the 3F4 binding site may comprise the entire loop four. Between F79 and Y93 a relatively conserved stretch of amino acids is predicted to form an α-helix that is covalently linked to β-strand two via disulfide bond C22-C83, consistent with an earlier proposal that this cluster of conserved amino acids may be important for the folding of more distal parts (Flomenberg et al., 1992). β-strand two forms another disulfide bond to the first loop (C28-C11). No conclusive suggestion can be made as to the relative orientation of the β-strands to each other (parallel/anti-parallel) and to the α-helix. However, the disulfide spacing suggests a rather compact structure for E3/19K.

The six β-strands may form two β-pleated sheets exhibiting an immunoglobulin-like fold. While the location of the cysteines and the disulfide bonds is clearly different to that in immunoglobulin light chains, immunoglobulin-like folds can obviously be created using variable cysteine arrangements, e.g. in the viral immune evasion protein US2 of human cytomegalovirus (Gewurz et al., 2001). Several other immune evasion proteins without significant sequence homology to immunoglobulins and with unusual disulfide bonds have recently been crystallized (Mans et al., 2007) and turned out to exhibit immunoglobulin-like folds. Fold recognition for the E3/19K lumenal domain using the Genesilico metaserver which covers methods such as Phyre, ffas, HHsearch, Mgenthreader or fugue gave no hits with statistically significant scores. Intriguingly though, amongst the hits with the highest scores, mostly coming from the SCOP "Immunoglobulin-like beta sandwich fold", are the α3 domain of HLA-B27 and beta 2 microglobulin, two proteins E3/19K interacts with. However, there is not sufficient evidence to postulate evolutionary or structural relatedness between the E3/19K lumenal domain and these proteins based on these data.

Apart from the structural insights and the possibility to assess the structural integrity of recombinant Ad2 E3/19K preparations for crystallisation or NMR analysis, we believe that the complement of mAbs now available will prove a valuable tool to enable detailed structure-function analyses of the Ad2 E3/19K protein. Combined with the Ctail antibody the expression level of mutated proteins can be standardised, a prerequisite for any functional analysis. Studies using alanine-scanning mutagenesis of all conserved amino acids are in progress to investigate whether or not the conformational changes identified here differentially affect the key functions of the E3/19K protein, namely binding and retention of MHC class I and MICA/B molecules, respectively. Support for distinct structural requirements for the modulation of MHC class I and the NK ligands MICA/B was provided by our recent study (McSharry et al., 2008), showing that alanine substitution of W96 in

E3/19K had little effect on MICA/B down regulation but essentially abolished HLA modulation. Thus, particular amino acids may be preferentially involved in interacting with MHC class I or MICA/B.

Considering that MICA/B serve as ligands for the NKG2D receptor which is not only expressed on NK cells but also present on human CD8 T cells, γ/δ T cells and NKT cells these studies have considerable implications for dissecting the immune evasion function of E3/19K.

Acknowledgements

We thank Dr Claudia Blindauer for helpful comments and Dr David Roper (both University of Warwick) for critically reading of the manuscript. The financial support by the DFG and Warwick University is gratefully acknowledged.

Figure legends (722)

Fig. 1. Specificity of mAbs for Ad2 E3/19K. (A) Immunoprecipitation of E3/19K from cell lysates of A549 cells that were either mock-infected (lanes 1-3), infected with Ad2 (lanes 4-6) or Ad5 (lanes 7-9) using mAb Tw1.3, 3A9 and 3F4. (B) Western blot showing the specificity of mAb 10A2 for Ad2 E3/19K. A549 cells were mock-infected (lanes 1 and 2), infected with Ad2 (lanes 3 and 4), or Ad5 (lanes 5 and 6). Lysates were precipitated with mAb Tw1.3 and precipitated material was separated on SDS-PAGE, blotted and probed with mAb 10A2. Samples were run under reducing (+DTT) and nonreducing (-DTT) conditions, respectively. The position of the E3/19K dimer is indicated.

Fig. 2. Minimal epitopes recognized by mAbs 10A2, 3A9 and 3F4. 49 13-mer peptides were synthesized on a cellulose membrane with an overlap of 11 amino acids. As peptides 23-49 did not give any positive results, only peptides 1-22 are shown. Asterisks on the left denote the peptides that reacted with the respective mAbs on the right. Underlined amino acids represent the minimal consensus sequences present in all peptides recognized by a particular mAb.

Fig. 3. Reactivity of mAbs with wild-type and cysteine replacement mutants of Ad2 E3/19K expressed in 293 cells. Cells indicated on top (numbers refer to the cysteine mutated) were metabolically labelled. Equal amounts of lysates were immunoprecipitated with the antibodies Ctail, Tw1.3, 3A9 and 3F4. After SDS-PAGE, the dried gel was exposed to X-Ray film (A-C). (A) Untransfected 293 cells (lanes 1-4); 293 cells transfected with wild-type E3/19K (293E3, lanes 5-8); mutant C11 (lanes 9-12) and C83 (lanes 13-16). (B) 293 transfectants expressing Ala-22 (lanes 1-4), C22 (lanes 5-8), and C28 (lanes 9-12). (C) 293 transfectants expressing C101 (lanes 1-4), C109 (lanes 5-8), and C122 (lanes 9-12).

Fig. 4. Relative binding of mAbs to cysteine replacement mutants of E3/19K. The amount of radioactive E3/19K precipitated by mAbs Tw1.3, 3A9, 3F4 and Ctail serum (see Fig. 3) was

quantitatively determined by PhosphoImager analysis. Relative binding of mAbs to the different mutants is expressed as the ratio of radioactivity precipitated by the mAbs versus Ctail. The ratio obtained for wild-type E3/19K was set to 1. Bars represent the mean of two independent experiments**.**

Fig. 5. Competition binding ELISA between mAbs 3A9, 3F4 and Tw1.3. His-E3/19K adsorbed on ELISA plates was pre-incubated with increasing amounts of unlabelled mAbs Tw1.3, 3A9, and 3F4 (0, 1, 2 and 5µg/well), followed by incubation with radiolabelled mAb Tw1.3 (A) and 3A9 (B), respectively. The amount of bound radioactive mAbs was determined and related to values without preincubation with unlabelled antibody (% of 0µg antibody/well). The results represent means of two independent experiments.

Fig. 6. Immunoprecipitation of glycosylated (-tunicamycin) and unglcosylated (+tunicamycin) Ad2 E3/19K protein. Cells were treated with tunicamycin (lanes 6-10) or were mock treated (lanes 1-5), and E3/19K was precipitated using the antibodies indicated above the lanes. Amounts of radioactivity in the E3/19K band were measured as explained in the legend to Fig. 3 and related to that obtained for the Ctail serum.

Fig. 7. Relative binding efficiency of mAbs to mutant forms of E3/19K containing alanine at the amino acid positions given below the graphs. Ctail serum was used as internal standard for each transfectant cell line. Binding to the different mutants (black bars) relative to wild-type E3/19K (white bar) was calculated as in legend to Fig. 4. Except for P9, I37 and V64 (tested once) each cell line was tested 2-4 times. The error bars represent the standard error of the mean.

Fig. 8. Annotated sequence alignment and predicted secondary structure for Ad2 E3/19K. For the clarity of representation and to avoid sequence redundancy the full sequence alignment of Ad2 and homologues was condensed to a subset representing all known subgroups. N-terminal signal peptides were truncated. The corresponding UniProt identifiers for the

sequences used in the alignment are: Q779F5 (Ad2), Q6VGT9 (Ad5), Q2KSH7 (Ad3), Q76Y41 (Ad35), Q67811 (Ad19a), Q7TBH1 (Ad8), Q2KSD9 (Ad4). For each sequence the respective Ad species is denoted in brackets. Fully conserved cysteine residues are highlighted in yellow, other conserved residues in grey. The results from three secondary structure prediction methods (jpred, psipred and predprot, see methods for details) are shown in three letter representation ("H" = helix, "E" = strand, "-" = coil). The two experimentally confirmed disulfide bridges are shown in the two bottom lines of the multiple sequence alignment, N-glycan attachment sites for Ad2 E3/19K are highlighted by an asterisk. The peptide epitopes of mAbs 3A9, 3F4 and 10A2 are indicated as grey blocks at the top of the figure.

References

Ahmed C. M., Chanda R. S., Stow N. D. and Zain B. S., 1982. The nucleotide sequence of mRNA for the Mr 19 000 glycoprotein from early gene block III of adenovirus 2. Gene 20, 339-346.

Altschul S. F., Gish W., Miller W., Myers E. W. and Lipman D. J., 1990. Basic Local Alignment Search Tool. J. Mol. Biol. 215, 403-410.

Andersson M., McMichael A. and Peterson P. A., 1987. Reduced allorecognition of adenovirus-2 infected cells. J. Immunol. 138, 3960-3966.

Beier D. C., Cox J. H., Vining D. R., Cresswell P. and Engelhard V. H., 1994. Association of human class I MHC alleles with the adenovirus E3/19K protein. J. Immunol. 152, 3862-3872.

Bennett E. M., Bennink J. R., Yewdell J. W. and Brodsky F. M., 1999. Cutting edge: adenovirus E19 has two mechanisms for affecting class I MHC expression. J. Immunol. 162, 5049-5052.

Bruder J. T., Jie T., McVey D. L. and Kovesdi I., 1997. Expression of gp19K increases the persistence of transgene expression from an adenovirus vector in the mouse lung and liver. J. Virol. 71, 7623-7628.

Bryson K., McGuffin L. J., Marsden R. L., Ward J. J., Sodhi J. S. and Jones D. T., 2005. Protein structure prediction servers at university college london. Nucleic Acids Research 33, W36-W38.

Burgert H.-G. and Blusch J. H., 2000. Immunomodulatory functions encoded by the E3 transcription unit of adenoviruses. Virus Genes 21, 13-25.

Burgert H.-G. and Kvist S., 1985. An adenovirus type 2 glycoprotein blocks cell surface expression of human histocompatibility class I antigens. Cell 41, 987-997.

Burgert H.-G. and Kvist S., 1987. The E3/19K protein of adenovirus type 2 binds to the domains of histocompatibility antigens required for CTL recognition. EMBO J. 6, 2019-2026.

Burgert H.-G., Maryanski J. L. and Kvist S., 1987. "E3/19K" protein of adenovirus type 2 inhibits lysis of cytolytic T lymphocytes by blocking cell-surface expression of histocompatibility class I antigens. Proc. Natl. Acad. Sci. U.S.A. 84, 1356-1360.

Burgert H.-G., Ruzsics Z., Obermeier S., Hilgendorf A., Windheim M. and Elsing A., 2002. Subversion of host defense mechanisms by adenoviruses. Curr. Top. Microbiol. Immunol. 269, 273-318.

Cole C., Barber J. D. and Barton G. J., 2008. The Jpred 3 secondary structure prediction server. Nucleic Acids Research 36, in press.

Cox J. H., Bennink J. R. and Yewdell J. W., 1991. Retention of adenovirus E19 glycoprotein in the endoplasmic reticulum is essential to its ability to block antigen presentation. J. Exp. Med. 174, 1629-1637.

Deryckere F. and Burgert H.-G., 1996. Early region 3 of adenovirus type 19 (subgroup D) encodes an HLA-binding protein distinct from that of subgroups B and C. J. Virol. 70, 2832-2841.

Edgar R. C., 2004. MUSCLE: multiple sequence alignment with high accuracy and high throughput. Nucl. Acids Res. 32, 1792-1797.

Elsing A. and Burgert H.-G., 1998. The adenovirus E3/10.4K-14.5K proteins down-modulate the apoptosis receptor Fas/Apo-1 by inducing its internalization. Proc. Natl. Acad. Sci. U.S.A. 95, 10072-10077.

Feuerbach D., Etteldorf S., Ebenau-Jehle C., Abastado J. P., Madden D. and Burgert H.-G., 1994. Identification of amino acids within the MHC molecule important for the interaction with the adenovirus protein E3/19K. J. Immunol. 153, 1626-1636.

Flomenberg P., Gutierrez E. and Hogan K., 1994. Identification of class I MHC regions which bind to the adenovirus E3-19k protein. Mol. Immunol. 31, 1277-1284.

Flomenberg P., Szmulewicz J., Gutierrez E. and Lupatkin H., 1992. Role of the adenovirus E3-19k conserved region in binding major histocompatibility complex class I molecules. J. Virol. 66, 4778-4783.

Fox J. P., Hall C. E. and Cooney M. K., 1977. The Seattle Virus Watch. VII. Observations of adenovirus infections. Am. J. Epidemiol. 105, 362-386.

Gabathuler R., Levy F. and Kvist S., 1990. Requirements for the association of adenovirus type 2 E3/19K wild-type and mutant proteins with HLA antigens. J. Virol. 64, 3679-3685.

Gewurz B. E., Gaudet R., Tortorella D., Wang E. W., Ploegh H. L. and Wiley D. C., 2001. Antigen presentation subverted: Structure of the human cytomegalovirus protein US2 bound to the class I molecule HLA-A2. Proc. Natl. Acad. Sci. USA 98, 6794-6799.

Ginsberg H. S., Lundholm Beauchamp U., Horswood R. L., Pernis B., Wold W. S., Chanock R. M. and Prince G. A., 1989. Role of early region 3 (E3) in pathogenesis of adenovirus disease. Proc. Natl. Acad. Sci. U.S.A. 86, 3823-3827.

Hermiston T. W., Tripp R. A., Sparer T., Gooding L. R. and Wold W. S., 1993. Deletion mutation analysis of the adenovirus type 2 E3-gp19K protein: identification of sequences within the endoplasmic reticulum lumenal domain that are required for class I antigen binding and protection from adenovirus-specific cytotoxic T lymphocytes. J.Virol. 67, 5289-5298.

Hilgendorf A., Lindberg J., Ruzsics Z., Höning S., Elsing A., Löfqvist M., Engelmann H. and Burgert H.-G., 2003. Two distinct transport motifs in the adenovirus E3/10.4-14.5 proteins act in concert to down-modulate apoptosis receptors and the epidermal growth factor receptor. J. Biol. Chem. 278, 51872-51884.

Jackson M. R., Nilsson T. and Peterson P. A., 1990. Identification of a consensus motif for retention of transmembrane proteins in the endoplasmic reticulum. EMBO J. 9, 3153-3162.

Jackson M. R., Nilsson T. and Peterson P. A., 1993. Retrieval of transmembrane proteins to the endoplasmic reticulum. J. Cell Biol. 121, 317-333.

Jefferies W. A. and Burgert H.-G., 1990. E3/19K from adenovirus 2 is an immunosubversive protein that binds to a structural motif regulating the intracellular transport of major histocompatibility complex class I proteins. J. Exp. Med. 172, 1653-1664.

Köhler G. and Milstein C., 1975. Continuous cultures of fused cells secreting antibody of predefined specificity. Nature 256, 495-497.

Körner H., Fritzsche U. and Burgert H.-G., 1992. Tumor necrosis factor alpha stimulates expression of adenovirus early region 3 proteins: implications for viral persistence. Proc. Natl. Acad. Sci. U.S.A. 89, 11857-11861.

Kornfeld R. and Wold W. S., 1981. Structures of the oligosaccharides of the glycoprotein coded by early region E3 of adenovirus 2. J. Virol. 40, 440-449.

Krogh A., Larsson B., von Heijne G. and Sonnhammer E. L. L., 2001. Predicting transmembrane protein topology with a hidden Markov model: Application to complete genomes. J. Mol. Biol. 305, 567-580.

Kurowski M. A. and Bujnicki J. M., 2003. GeneSilico protein structure prediction meta-server. Nucl. Acids Res. 31, 3305-3307.

Lichtenstein D. L., Toth K., Doronin K., Tollefson A. E. and Wold W. S., 2004. Functions and mechanisms of action of the adenovirus E3 proteins. Int. Rev. Immunol. 23, 75-111.

Liu H., Fu J. and Bouvier M., 2007. Allele- and Locus-Specific Recognition of Class I MHC Molecules by the Immunomodulatory E3-19K Protein from Adenovirus. J. Immunol. 178, 4567-4575.

Liu H., Stafford W. F. and Bouvier M., 2005. The endoplasmic reticulum lumenal domain of the adenovirus type 2 E3-19K protein binds to peptide-filled and peptide-deficient HLA-A*1101 molecules. J. Virol. 79, 13317-13325.

Lodoen M. B. and Lanier L. L., 2005. Viral modulation of NK cell immunity. Nat. Rev. Micro. 3, 59-69.

Mans J., Natarajan K., Balbo A., Schuck P., Eikel D., Hess S., Robinson H., Simic H., Jonjic S., Tiemessen C. T. and Margulies D. H., 2007. Cellular Expression and Crystal Structure of the Murine Cytomegalovirus Major Histocompatibility Complex Class I-like Glycoprotein, m153. J. Biol. Chem. 282, 35247-35258.

McNees A. L. and Gooding L. R., 2002. Adenoviral inhibitors of apoptotic cell death. Virus Res. 88, 87-101.

McSharry B., Burgert H.-G, Owen D. P., Stanton R., Prod'homme V., Sester M., Koebernick K., Groh V., Spies T., Cox S., Little A. M., Wang E. C., Tomasec P. and Wilkinson G. W., 2008. Adenovirus E3/19K Promotes Evasion of NK Cell Recognition by Intracellular Sequestration of the NKG2D Ligands MICA and MICB. J. Virol. 80, in press.

Nilsson T., Jackson M. and Peterson P. A., 1989. Short cytoplasmic sequences serve as retention signals for transmembrane proteins in the endoplasmic reticulum. Cell 58, 707-718.

Pääbo S., Bhat B. M., Wold W. S. and Peterson P. A., 1987. A short sequence in the COOH-terminus makes an adenovirus membrane glycoprotein a resident of the endoplasmic reticulum. Cell 50, 311-317.

Pääbo S., Nilsson T. and Peterson P. A., 1986a. Adenoviruses of subgenera B, C, D, and E modulate cell-surface expression of major histocompatibility complex class I antigens. Proc. Natl. Acad. Sci. U.S.A. 83, 9665-9669.

Pääbo S., Weber F., Nilsson T., Schaffner W. and Peterson P. A., 1986b. Structural and functional dissection of an MHC class I antigen-binding adenovirus glycoprotein. EMBO J. 5, 1921-1927.

Persson H., Jansson M. and Philipson L., 1980. Synthesis and genomic site for an adenovirus type 2 early glycoprotein. J. Mol. Biol. 136, 375-394.

Rawle F. C., Tollefson A. E., Wold W. S. and Gooding L. R., 1989. Mouse anti-adenovirus cytotoxic T lymphocytes. Inhibition of lysis by E3 gp19K but not E3 14.7K. J. Immunol. 143, 2031-2037.

Rost B., Fariselli P. and Casadio R., 1996. Topology prediction for helical transmembrane proteins at 86% accuracy. Protein Science 5, 1704-1718.

Rost B. and Sander C., 1993. Prediction of Protein Secondary Structure at Better than 70% Accuracy. J. Mol. Biol. 232, 584-599.

Rost B., Yachdav G. and Liu J. F., 2004. The PredictProtein server. Nucl. Acids Res. 32, W321-W326.

Sester M. and Burgert H.-G., 1994. Conserved cysteine residues within the E3/19K protein of adenovirus type 2 are essential for binding to major histocompatibility complex antigens. J. Virol. 68, 5423-5432.

Sester M., Feuerbach D., Frank R., Preckel T., Gutermann A. and Burgert H.-G., 2000. The amyloid precursor-like protein 2 associates with the major histocompatibility complex class I molecule K(d). J. Biol. Chem. 275, 3645-3654.

Tanaka Y. and Tevethia S. S., 1988. Differential effect of adenovirus 2 E3/19K glycoprotein on the expression of H-2Kb and H-2Db class I antigens and H-2Kb- and H-2Db-restricted SV40-specific CTL-mediated lysis. Virology 165, 357-366.

The_UniProt_Consortium. 2007. The Universal Protein Resource (UniProt). Nucl. Acids Res. 35, D193-D197.

von Herrath M. G., Efrat S., Oldstone M. B. and Horwitz M. S., 1997. Expression of adenoviral E3 transgenes in beta cells prevents autoimmune diabetes. Proc. Natl. Acad. Sci. U.S.A. 94, 9808-9813.

Windheim M., Hilgendorf A. and Burgert H.-G., 2004. Immune evasion by adenovirus E3 proteins: exploitation of intracellular trafficking pathways. Curr. Top. Microbiol. Immunol. 273, 29-85.

Wold W. S., Cladaras C., Deutscher S. L. and Kapoor Q. S., 1985. The 19-kDa glycoprotein coded by region E3 of adenovirus. Purification, characterization, and structural analysis. J. Biol. Chem. 260, 2424-2431.

Wold W. S. M. and Horwitz M. S. (2007) Adenoviruses. In *Fields Virology* (Edited by Knipe D. M., Howley P. M., Griffin D. E. and Lamb R. A.), p. 2395-2436. Lippincott Williams & Wilkins.

Table 1

Properties of E3/19K-specific monoclonal antibodies

Name[a]	Isotype[b]	Minimal epitope[c]	crucial aa[d]	IP[e]	Western blot[f] nred	Western blot[f] red	FACS, IF[g]	unfolded[h]
10A2	IgG1	3-13	E^{5}	-	+	+++	+/-	++
3A9	IgG1	15-21	K^{16}, S^{17}	+++	++	+/-	+++	++
3F4	IgG1	41-45	D^{41}, K^{42}	+	+	+++	+	+++
Tw1.3[i]	IgG3	disc.	I^{37}, V^{64} I^{26}, $K^{42,}$	+++	++	-	+++	-

The name of the mAbs and the isotype is given under (a) and (b), respectively. The minimal epitope in (c) was determined by scanning a corresponding peptide library. The most crucial amino acids in each epitope are indicated in (d, see text for further explanation). For 3A9 and Tw1.3 also the cysteines in position 11 and 28 are absolutely essential. Columns in e-h summarize the results obtained with these mAbs in immunoprecipitation (e), Western blots (f) under non-reducing (nred) and reducing (red) conditions, as well as in FACS (g) and immunofluorescence (IF), differentiating between strong (+++), average (++), low (+) and little/minimal (+/-) or no signal (-) when detecting wild-type E3/19K. Column (h) indicates the ability of the mAb to recognize unfolded or partially unfolded E3/19K mutants. Tw1.3 (Cox et al., 1991) has a discontinuous epitope (disc) with the most critical amino acids (aa) indicated.

Figure 1

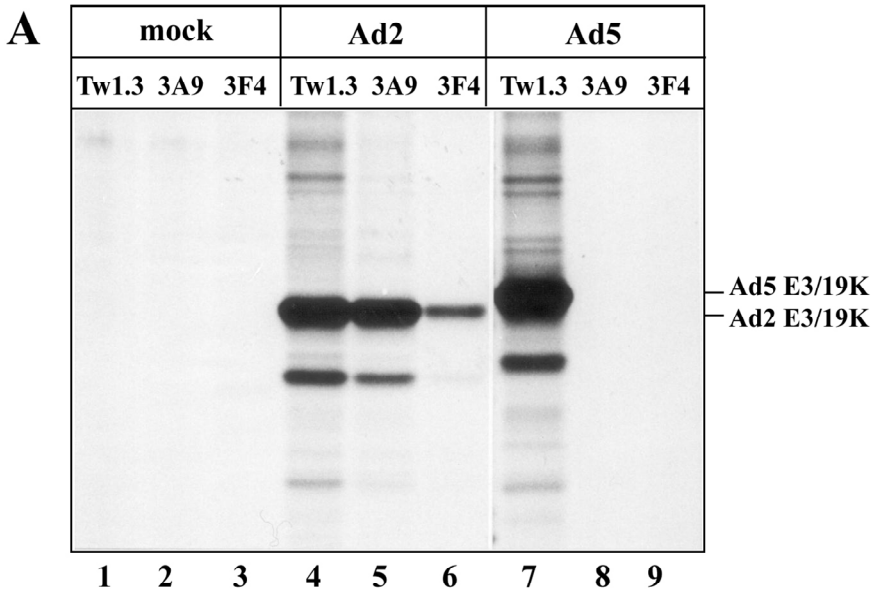
A
mock
Ad2
Ad5
Tw1.3 3A9 3F4 Tw1.3 3A9 3F4 Tw1.3 3A9 3F4
Ad5 E3/19K
Ad2 E3/19K
1 2 3 4 5 6 7 8 9

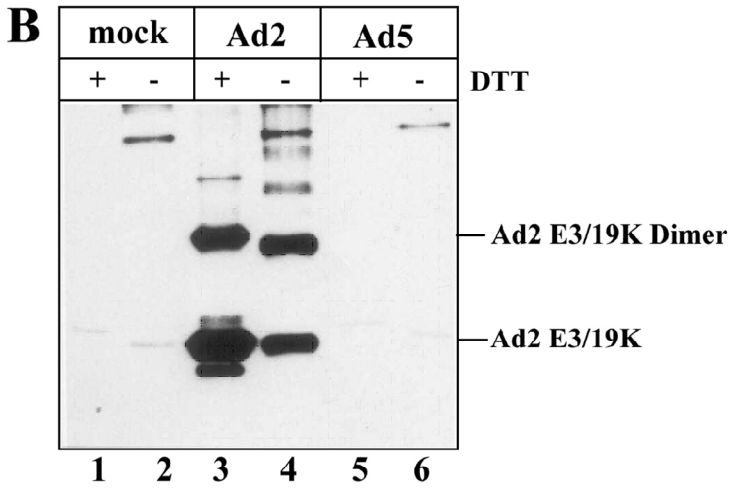
B
mock
Ad2
Ad5
+ - + - + -
DTT
Ad2 E3/19K Dimer
Ad2 E3/19K
1 2 3 4 5 6

Figure 2

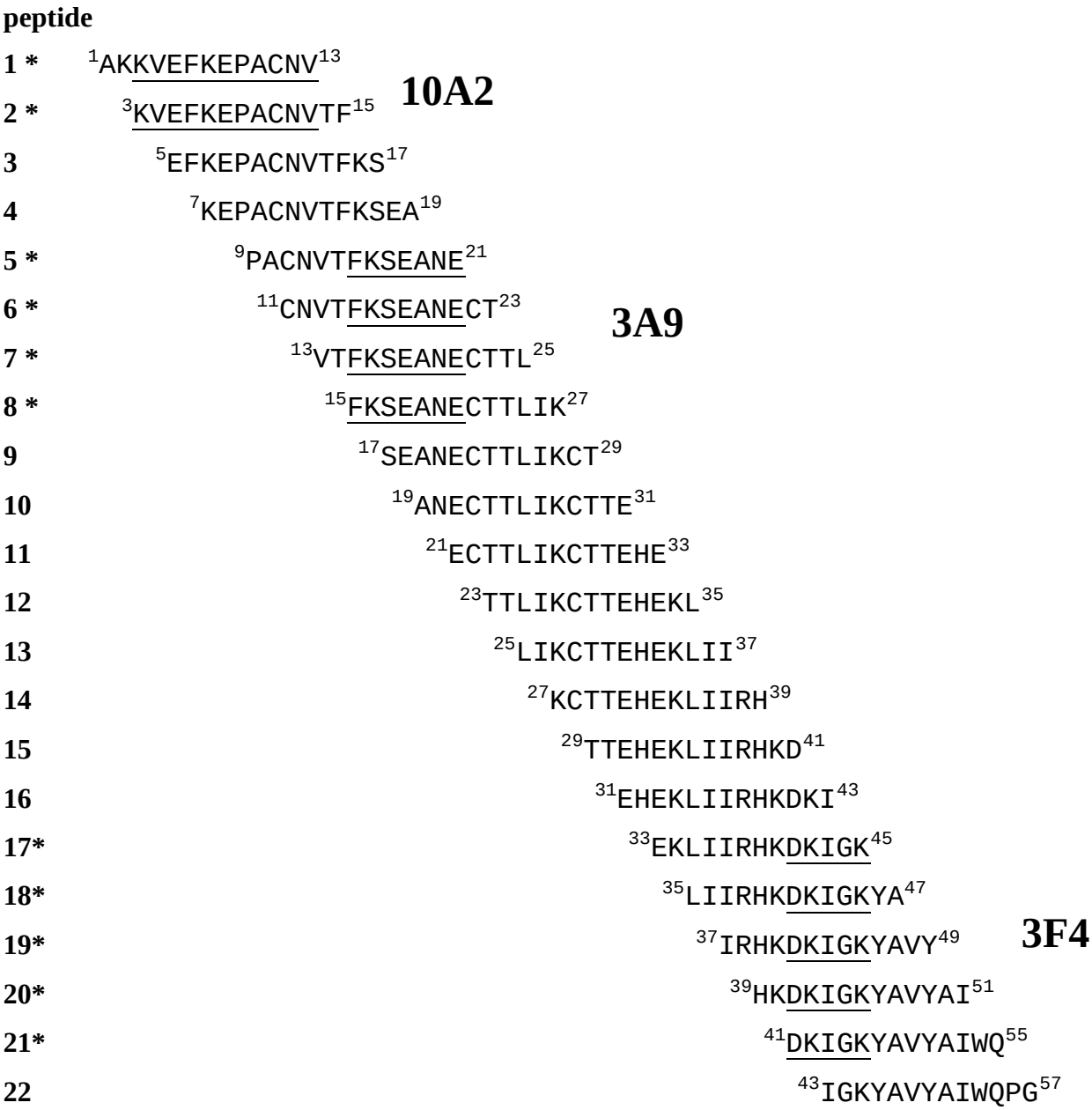
peptide
1 * 1AKKVEFKEPACNV13
2 * 3KVEFKEPACNVTF15
3 5EFKEPACNVTFKS17
4 7KEPACNVTFKSEA19
5 * 9PACNVTFKSEANE21
6 * 11CNVTFKSEANECT23
7 * 13VTFKSEANECTTL25
8 * 15FKSEANECTTLIK27
9 17SEANECTTLIKCT29
10 19ANECTTLIKCTTE31
11 21ECTTLIKCTTEHE33
12 23TTLIKCTTEHEKL35
13 25LIKCTTEHEKLII37
14 27KCTTEHEKLIIRH39
15 29TTEHEKLIIRHKD41
16 31EHEKLIIRHKDKI43
17* 33EKLIIRHKDKIGK45
18* 35LIIRHKDKIGKYA47
19* 37IRHKDKIGKYAVY49
20* 39HKDKIGKYAVYAI51
21* 41DKIGKYAVYAIWQ55
22 43IGKYAVYAIWQPG57
10A2
3A9
3F4

Figure 3

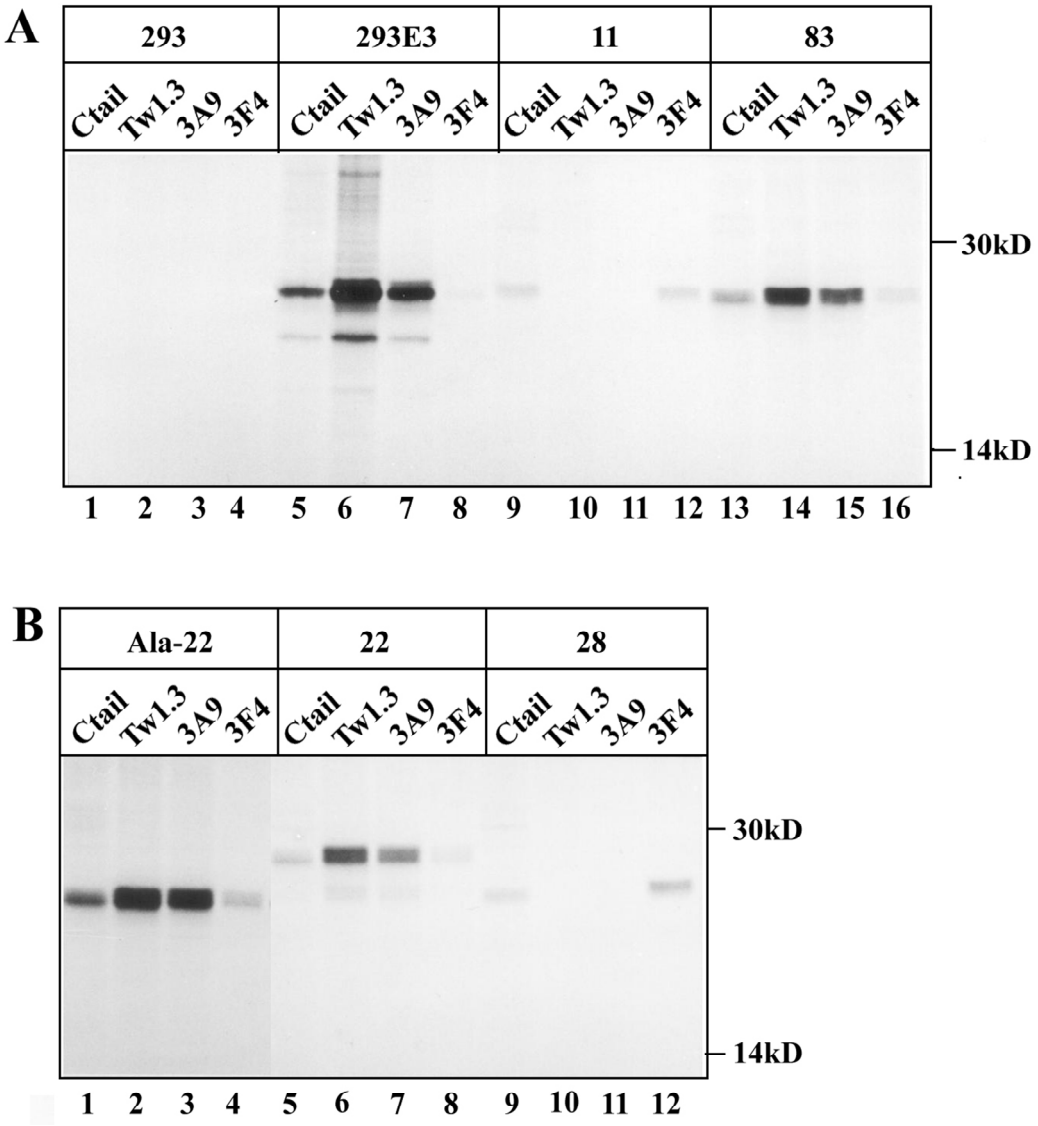
A
293
293E3
11
83
Ctail
Tw1.3
3A9
3F4
30kD
14kD
1 2 3 4 5 6 7 8 9 10 11 12 13 14 15 16
B
Ala-22
22
28
Ctail
Tw1.3
3A9
3F4
30kD
14kD
1 2 3 4 5 6 7 8 9 10 11 12
C
101
109
122
Ctail
Tw1.3
3A9
3F4
30kD
1 2 3 4 5 6 7 8 9 10 11 12

Figure 4

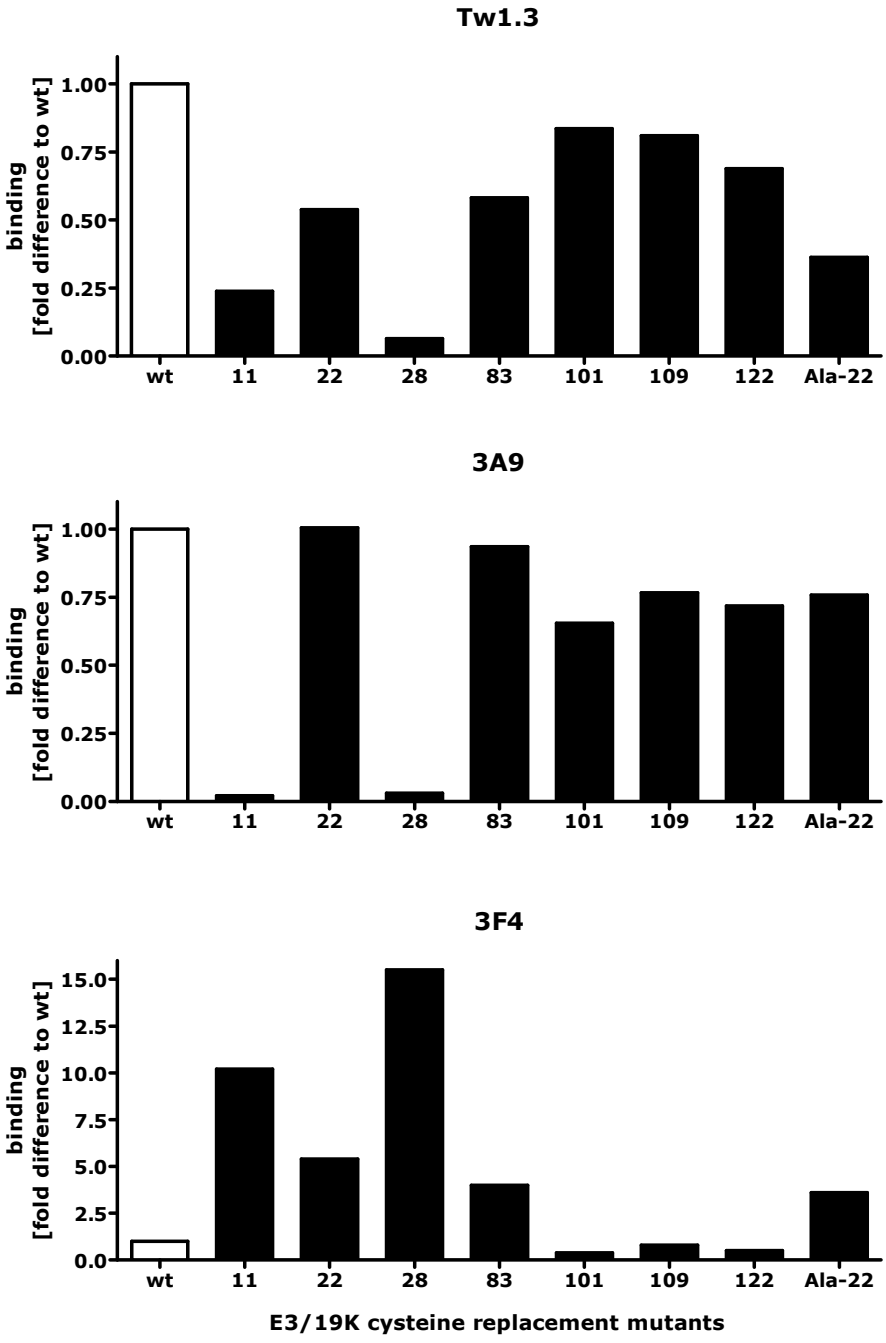
Tw1.3
binding [fold difference to wt]
1.00
0.75
0.50
0.25
0.00
wt
11
22
28
83
101
109
122
Ala-22
3A9
binding [fold difference to wt]
1.00
0.75
0.50
0.25
0.00
wt
11
22
28
83
101
109
122
Ala-22
3F4
binding [fold difference to wt]
15.0
12.5
10.0
7.5
5.0
2.5
0.0
wt
11
22
28
83
101
109
122
Ala-22
E3/19K cysteine replacement mutants

Figure 5

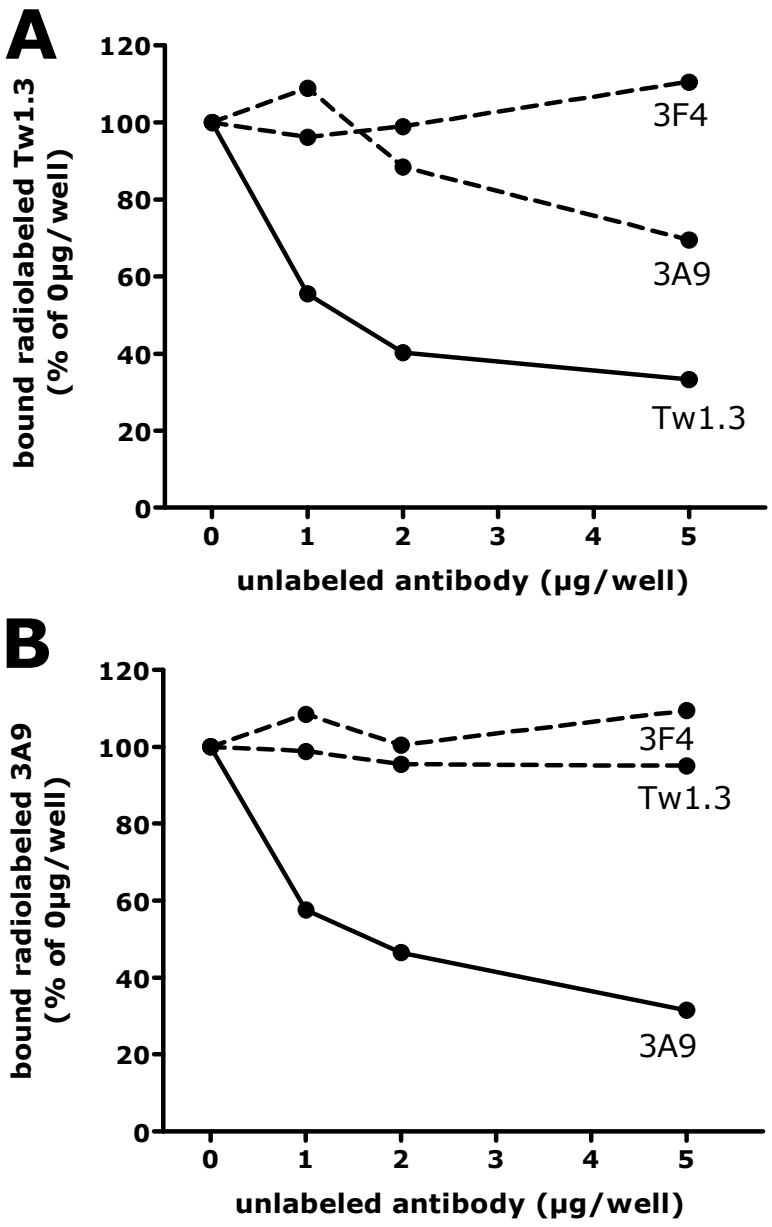
A
bound radiolabeled Tw1.3
(% of 0µg/well)
120
100
80
60
40
20
0
0
1
2
3
4
5
unlabeled antibody (µg/well)
3F4
3A9
Tw1.3
B
bound radiolabeled 3A9
(% of 0µg/well)
120
100
80
60
40
20
0
0
1
2
3
4
5
unlabeled antibody (µg/well)
3F4
Tw1.3
3A9

Figure 6

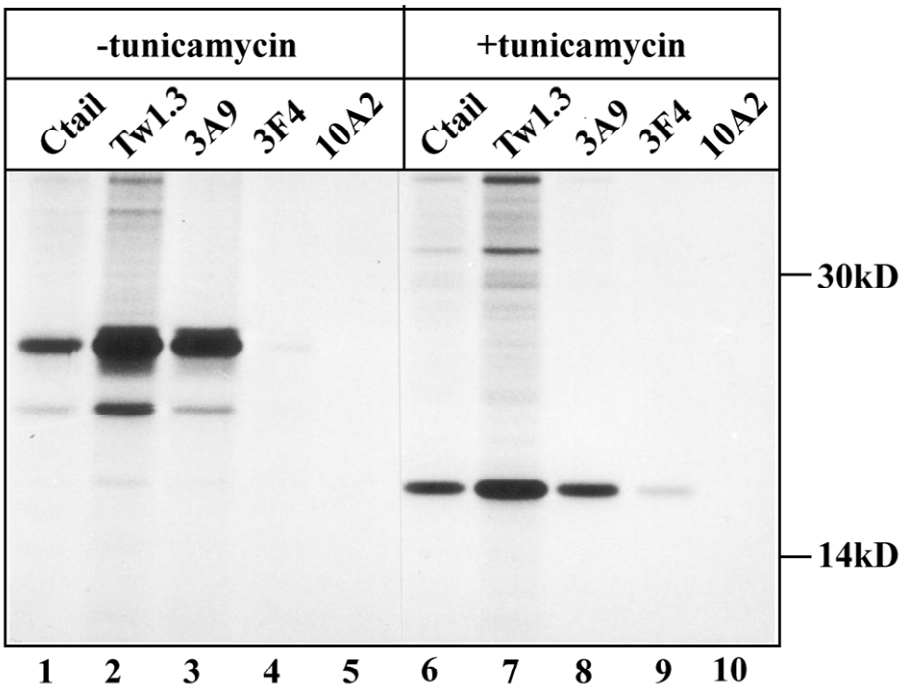
-tunicamycin
+tunicamycin
Ctail
Tw1.3
3A9
3F4
10A2
Ctail
Tw1.3
3A9
3F4
10A2
30kD
14kD
1
2
3
4
5
6
7
8
9
10

Figure 7

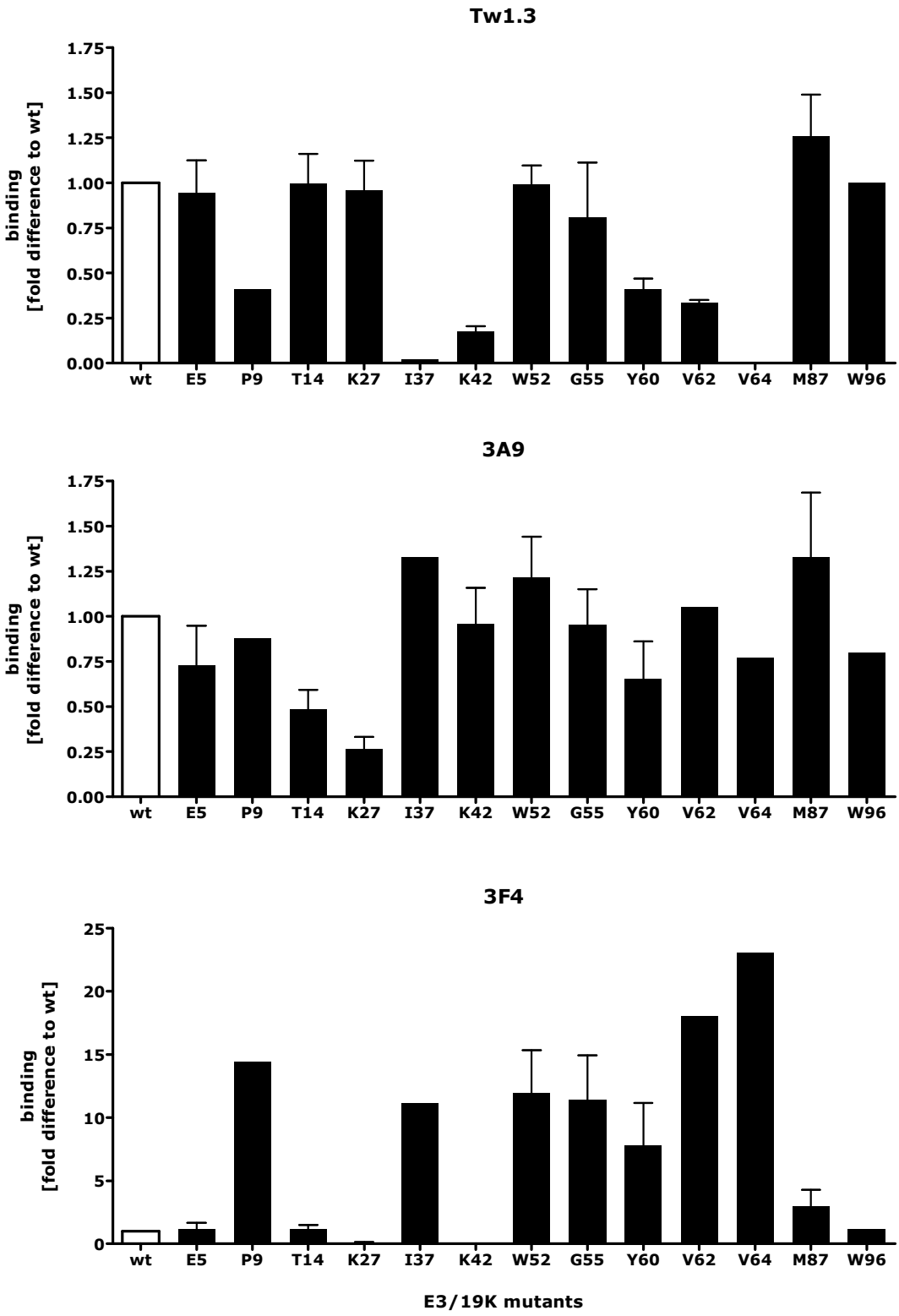
Tw1.3
binding
[fold difference to wt]
1.75
1.50
1.25
1.00
0.75
0.50
0.25
0.00
wt E5 P9 T14 K27 I37 K42 W52 G55 Y60 V62 V64 M87 W96
3A9
binding
[fold difference to wt]
1.75
1.50
1.25
1.00
0.75
0.50
0.25
0.00
wt E5 P9 T14 K27 I37 K42 W52 G55 Y60 V62 V64 M87 W96
3F4
binding
[fold difference to wt]
25
20
15
10
5
0
wt E5 P9 T14 K27 I37 K42 W52 G55 Y60 V62 V64 M87 W96
E3/19K mutants


10A2
3A9
3F4
Ad2 (C) AKKVEFKEPACNVTFKSEAN-ECTTLIKCTTEHEKLIIRHKDKIGKYAVYAIWQPGDTNDYNVTVFQGENR-K
jpred ----------EEEE------EEEEEEEE----EEEEEEE-----EEEEE-------EEEEEEE-----E
psipred ----------EEEE------EEEEEEE-----EEEEE-------EEEE--------EEEEE-------
predprot ----------EEEE------EEEEEEE-----EEEEE-------EEEE---------EEEE-------
Ad5 (C) TQKVDFKEPACNVTFAAEAN-ECTTLIKCTTEHEKLLIRHKNKIGKYAVYAIWQPGDTTEYNVTVFQGKSH-K
Ad3 (B1) DPCLDFDPENCTLTFAPDTSRLCGVLIKCGWDCRFVEITHNNKTWNNTLSTTWEPGVPEWYTVSVRGPDGSIR
Ad35 (B2) DPCLDFDPENCTLTFAPDTSRICGVLIKCGWECRSVEITHNNKTWNNTLSTTWEPGVPEWYTVSVRGPDGSIR
Ad19a (D) GVLSCHEQPRCNITTGNERN-DCSVVIKCEHHC-PLNITFKNKTMGNVWVGFWQPGDEQNYTVTVHGSNGN-H
Ad8 (D) GVLSCHEQPRCNITTGNERSIICTVVIKCEHKC-PLNITFKNRTMGNAWVGDWKPGDEQNYTVTVHGSNGN-H
Ad4 (E) DPCLTFNPDKCQLSFQPDGN-RCAVLIKCGWECDSVVIHYKNKTRNNTLASTWQPGDPEWYTVSVPGADGSLR
S----------+-----S
*
S----------
*
Ad2 (C) TFMYKFPFYEMCDITMYMSKQYKLWPP--QKCLENTGTFCSTALLITALALVCTLLYLKYKSRRSFIDEKKMP
jpred EE-----HHHHHHHHHHHHH--------------HHHHHHHHHHHHHHHHHHHHHHHHH----------
psipred EE--EEEHHHHHHHHHHHHHH-------------EEEEEHHHHHHHHHHHHHHHHEEE-------HH----
predprot EEEEEEEE--HHHHHHHHHHHH-------------EEEEHHHHHHHHHHHHHHHHEEEE----HHHH----
Ad5 (C) TFMYTFPFYEMCDITMYMSKQYKLWPP--QNCVENTGTFCCTAMLITVLALVCTLLYIKYKSRRSFIEEKKMP
Ad3 (B1) ISNNTFIFSEMCDLAMFMSRQYDLWPPSKENIVAFSIAYCLVTCIITAIICVCIHLLIVIRPRQSNEEKEKMP
Ad35 (B2) ISNNTFIFSEMCDLAMFMSKQYSLWPPSKDNIVTFSIAYCLCACLLTALLCVCIHLLVTTRIKNAN-NKEKMP
Ad19a (D) TFGFKFIFEVMCDITLHVARLHGLWPPTKDNMVGFSLAFVIMACLMSGLLVGALVWFLKRKPRYGNEEKEKLL
Ad8 (D) TFGFKFIFEVMCDITLHVARLHGLWPPTKKNMVGFSLAFVIMACFMSGLLVGALVWFLKRKPRYGNEEKEKLL
Ad4 (E) TVNNTFIFKHMCNTAMFMSRQYDMWPPRKENIVVFSIAYSLCTVLITAIVCLSIHMLIAIRPRNNA-EKEKQP
|
----------S